Novel high-temperature, high-power handling all-Cu interconnections through low-temperature sintering of nanocopper foams

Ninad Shahane, Kashyap Mohan, Pulugurtha Markondeya Raj, Vanessa Smet, and Rao Tummala
3D Systems Packaging Research Center
Georgia Institute of Technology
Atlanta, GA USA
e-mail: ninad.shahane@gatech.edu

Antonia Antoniou, Rakesh Behera
School of Mechanical Engineering
Georgia Institute of Technology
Atlanta, GA USA
e-mail: antonia.antoniou@me.gatech.edu

***Abstract*—Direct Cu-Cu bonding has been pursued by the semiconductor industry as the next interconnection node, for its superior power-handling capability, thermal stability and reliability as compared to traditional solders. However, manufacturability of Cu interconnections has so far been severely limited by the relatively high modulus of Cu, requiring costly planarization processes to address non-coplanarities and warpage to enable bonding in solid-state. This paper introduces a new class of all-Cu interconnections formed by low-temperature sintering of low-modulus nanocopper foams. The physical properties of these foams are tunable with their nanostructure and morphology, giving design flexibility. The proposed nanocopper interconnections have the following advantages: 1) fabrication compatible with standard semiconductor infrastructures and processes; 2) sub-20GPa elastic modulus pre-sintering providing tolerance to non-coplanarities and warpage in assembly; 3) densification at temperatures below 250°C to form high-density all-Cu interconnections, with excellent electrical and thermal properties; and 4) wide applicability from ultra-fine pitch to large-area interconnections for high-power devices. This paper reports the fabrication, characterization and first proof-of-concept demonstration of sintering of such nanocopper interconnections. Nanocopper foams were first synthetized by co-sputtering 2µm $Cu_{25}Si_{75}$ (at%) thin films on Si(100) substrates, and then electrochemically dealloying the thin-films in hydrofluoric acid under a range of applied voltages. Imaging of the foams by scanning electron microscopy (SEM) confirmed that they consisted of 45nm-sized uniform copper ligaments. Further, native oxides present in the as-synthetized samples were effectively removed with a short etching step in acetic acid, as confirmed by X-ray photoelectron spectroscopy (XPS) analysis, without affecting the foams' nanostructure. Differential scanning calorimetry (DSC) characterization indicated an exothermal peak at 180°C, beyond which coarsening may initiate. Finally, isothermal aging of the nanofoams was carried out in N_2 atmosphere at 100 and 300°C range for 180-900sec. No sintering was observed after aging at 150°C, as expected from DSC results, while sintering was confirmed after only 180s at 300°C, with observed densification and shrinkage of the foam, successfully demonstrating the proposed concept. In conclusion, a novel nanocopper foam interconnection technology is demonstrated with the potential to address manufacturability, scalability and cost across consumer, high performance and automotive applications.**

Keywords - Nanocopper foam; nanoporous; coarsening; densification; interconnections; automotive electronics

I. INTRODUCTION

The growing demands for interconnection technologies with higher power-handling, electrical and thermal performance as well as reliability, in digital, analog, and automotive applications is expected to drive the impending elimination of solders. In the digital space, advances in high-performance computing with increasing transmission speed and bandwidth requirements, at lower power consumption, are bringing new packaging solutions, including 2.5D interposer packages and 3D IC integration. Such complex system integration relies on off-chip I/O pitches of 30µm and below, with subsequent increase in current densities, pushing the limits of the current Cu pillar technology [1]. Pitch scaling is also accompanied by a reduction in solder volume, raising severe reliability concerns. A similar push for high-current density interconnections is observed in current analog applications. Further, interconnection technologies with thermal stability at temperatures above 250°C are also sought after in automotive applications with the multiplication of under-the-hood electronic systems. Standard SAC alloys cannot survive such high operating temperatures, while the use of high-temperature lead-free alloys, typically with a high Au content, is hindered by the high cost of Au, writing solders off as potential candidates for high-temperature packaging [2].

Such electrical and thermal requirements have long existed in power electronics. Intensive research has been focused on alternative technologies such as diffusion soldering, including solid-liquid interdiffusion (SLID) [3] or transient liquid phase (TLP) [4] processes in various systems, as well as low-temperature sintering of nanosilver pastes [5, 6]. These technologies have been successfully implemented in limited volume manufacturing, with Infineon's recent Cu-Sn SLID in its IGBT power modules [7-9], and Semikron's known thrust in Ag sintering [10, 11]. Large-scale adoption of these emerging technologies, however, remains limited by manufacturability, reliability and cost concerns. In parallel, the digital space reached the same conclusions with the use of Cu-Sn SLID bonding in 3D ICs, recently demonstrated by IMEC with 3D stacking of DRAMs [12]. However, SLID technologies face their own challenges of high assembly cycle times, reliability

978-1-5090-1204-6/16 $31.00 © 2016 IEEE
DOI 10.1109/ECTC.2016.352

issues on account of kirkendall voiding and intermetallic brittleness [13].

Beyond SLID, pitch scaling has also been driving solid-state bonding technologies. Au-Au interconnections (GGI) were established by both thermocompression and ultrasonic bonding [14, 15], but their applicability is again limited by cost, despite their excellent overall performance. Copper, on the other hand, is relatively inexpensive, and has outstanding electrical and thermal conductivities, thermal stability, current-carrying capability, high-frequency performance and is compatible with standard back-end-of-line (BEOL) infrastructures [16, 17]. However, direct Cu-Cu bonding faces three fundamental challenges degrading manufacturability: 1) oxidation, 2) relatively low diffusivity of Cu at reasonable bonding temperatures, and 3) low tolerance to noncoplanarities in the absence of the low-modulus molten solder phase. Georgia Tech's Packaging Research Center (GT-PRC) recently pioneered low-temperature Cu interconnections, using ultra-thin Au-based metallic finishes to inhibit copper oxidation and form strong, reliable joints at temperatures below 200°C, significantly improving manufacturability [18]. The team is now exploring low-cost planarization techniques to further lower bonding pressures. In this regard, the use of nanocopper inks to form all-Cu interconnections by capillary bridging was recently proposed by IBM Zurich [19].

All applications seem to converge toward nanomaterials acting as a key enabler to achieve strong, reliable joints with high current-carrying capability and thermal stability at low bonding temperatures. Although the use of nano-inks or pastes has gained momentum in recent years, the technology readiness of sintering processes is still questioned [20], with the following arguments: 1) variations in paste compositions and processing leading to highly-customized assembly processes; 2) limited pitch scalability due to risks of bridging; 3) retained porosity post-sintering, giving microstructural instability and subsequent reliability concerns; and 4) stress management issues with stiff interconnections. Nanocopper pastes are currently in development by several manufacturers like Lockheed Martin, Indium or Namics [21, 22], but face an additional challenge related to expensive surface treatments of Cu nanoparticles to prevent oxidation, thus overruling the cost benefits of copper. A new class of copper interconnections, with the same performance as Ag sintering but the processability of solders, at low cost, is thus required to solve this grand challenge.

GT-PRC proposes nanocopper foams as a breakthrough technology platform to form unique Cu interconnections by solid state-sintering at temperatures below 250°C. These nanofoams are essentially metallic sponge-like materials, at nanoscale. In the literature they can be referred as Nanoporous (NP) metals, a class of open-cell foams with ligaments and pores at the nanoscale. Unlike bulk foam synthesis work, the most commonly used synthesis technique is by dealloying or selective etching of an alloy in a corrosive environment. Under certain conditions, it is possible that the remnant solid fraction of the alloy self-assembles into a three dimensional interconnected network of ligaments at the nanoscale [23-31]. Over the past decade, a variety of other nanoporous metals have been synthesized [24, 25, 29, 32-44]. NP metals have been proposed in a variety of applications ranging from catalysis [45-52], sensors, actuators, microfluidic controllers and so forth [53]. Similarly, the precursor alloy can be obtained from a range of techniques including sputtering, electrolytic plating or high temperature alloying, followed by a dealloying step [54-59]. The resulting NP metal interconnections can be formed and patterned directly on wafers or substrates, or as preform materials. Nanocopper foam physical properties vary with alloying composition, density, dealloying conditions and morphology, and can therefore be tuned to any application needs. Isotropic or transversely isotropic (e.g. columnar) nanofoams can introduce additional design flexibility by reducing lateral stresses [41, 60]. Copper ligaments below 25nm in length are extremely reactive on account of higher surface-to-volume ratio, thus enabling sintering and densification of the nanocopper foam and simultaneous strong metallurgical bonding at temperatures below 250°C [61]. The sub-20GPa modulus of these foams [62] is 6x lower than that of bulk copper and allows for some compensation of die/substrate non-coplanarities and warpage, improving assembly manufacturability. These Cu nanofoams can, for example, replace the solder cap from traditional Cu pillar interconnections as illustrated in Fig. 1, bringing compliance to direct Cu-Cu bonding while maintaining pitch scalability. This novel approach to solid-state all-Cu interconnections thus has the potential to meet the specific electrical, thermal and reliability needs of a variety of applications, ranging from consumer, high-performance to automotive, while addressing challenges such as manufacturability, scalability and cost.

This paper constitutes an initial proof-of-concept of nanocopper foam interconnections. Amorphous Cu-Si films were fabricated by co-sputtering and subsequent dealloying to produce isotropic nanocopper foams with ligament sizes in the 45nm target range. The composition before and after dealloying was characterized through XPS analysis. XPS analysis was further used to qualitatively characterize the removal of native oxides from the surface of the as-dealloyed nanocopper foam. DSC characterization was carried out to identify critical temperatures for onset of coarsening. A preliminary study of the sintering of nanocopper foams was conducted by isothermal aging in the 100-300°C range. Resulting shrinkage from densification was finally evaluated for each of the samples

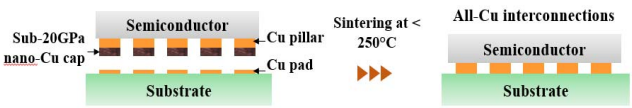

Figure 1. New GT-PRC concept: Cu pillar with nanocopper foam cap.

II. NANOFOAM FABRICATION AND CHARACTERIZATION

A. Copper Nanofoam Synthesis

Nanocopper foams were synthesized through a two-step process. First, thin films of amorphous copper silicide of $Cu_{0.25}Si_{0.75}$ composition by atomic percent were co-sputtered by physical vapor deposition (PVD) on a (100)-oriented Si wafer to a thickness of 2µm. The composition of the initial alloy was ascertained through XPS analysis. A scanning electron microscopy (SEM) micrograph of the as-deposited $Cu_{0.25}Si_{0.75}$ film is shown in Fig. 2(a), for reference. The original wafer was cleaved and each sample was dealloyed in 3% hydrofluoric acid in distilled water, in ambient conditions. Hydrofluoric acid can also react with the Si substrate, potentially causing delamination of the Si substrate-to-amorphous alloy interface during the dealloying process. To prevent this, a thin polymeric film, non-reactive with hydrofluoric acid, was applied on all sides but the top surface of each sample. Dealloying commences from the free surface and proceeds through the thickness of the foam. As the dealloying front progresses through the thickness, the silicon dissolves in the electrolyte. At the same time, the majority of the copper self assembles into a three dimensional network of ligaments. The electrochemical dealloying was performed with a three-electrode system consisting of the precursor alloy as working electrode, a saturated calomel electrode (SCE) as reference electrode, and a Pt counter electrode. The samples were dealloyed under fixed external voltage of -0.3V for 300sec. It has been shown that the morphology of metallic foams strongly depends on the applied dealloying potential [63, 64]. The samples were characterized with plan and cross-section (90º tilt) SEM views in several locations, and at various magnifications, by Field Emission Scanning Electron Microscopy (FE-SEM) using a Zeiss Ultra60 scanning electron microscope as can be seen in Fig. 2.

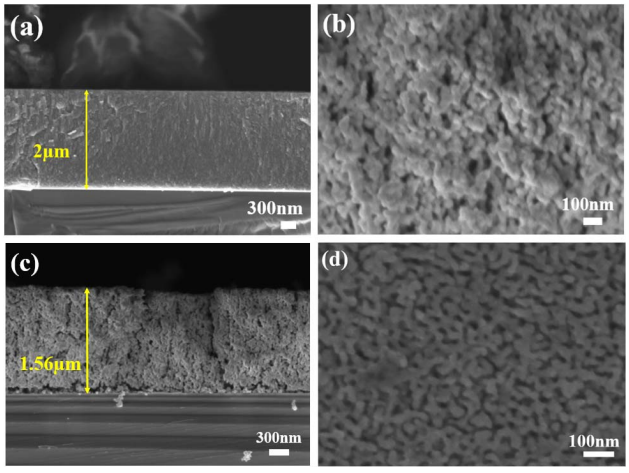

Figure 2. SEM micrographs of (a) 90º tilt view of as-sputtered precursor $Cu_{0.25}Si_{0.75}$ thin-film on Si substrate, (b) 90º tilt view of nanocopper foam formed after dealloying, (c) 90º tilt view of the nanocopper foam coverage across the Si substrate, (d) plan-view of nanocopper foam.

The fabricated foams feature an isotropic open cell structure, with an average ligament thickness of 45nm over 25 measurements, as can be seen in Fig. 2(b). Fig. 2(c) shows excellent homogeneity and isotropy of the nanocopper foam across the length of the Si substrate. It was confirmed through a combination of XPS and ion milling that the synthesized nanocopper foams contained no remnant silicon to within the resolution limit of the technique (0.1% by atom). A reduction in height of the nanocopper foam films from the initial 2µm copper silicide thickness to 1.56µm was observed, due to shrinkage during dealloying. Dealloying for longer times results in higher shrinkage of the foams, and brings about coarsening and thickening of the ligaments [58].

B. Oxidation of Nanocopper Foams

Oxidation is a major concern in copper processing. It is well known that on exposure to air, copper oxidizes and forms a mixed oxide film of thermodynamically stable Cu_2O, CuO, $Cu(OH)_2$, chemisorbed water and carboxylate species [65]. At room temperature, these oxides are self-limiting and form a passive barrier over the Cu surface. Metallurgical bonding typically requires clean and oxide-free surfaces for highest interdiffusion rates. Oxidation kinetics in nano-scale Cu are less understood. It is therefore critical to gain a fundamental understanding of this process in nanocopper foams, and explore solutions to break this layer of surface oxides. Acetic acid has been demonstrated very effective in removing native oxides from the surface of copper thin-films. Acetic acid reacts with copper oxides to form cupric acetate, without reacting with metallic copper, through the following reactions:

$$CuO + 2CH_3COOH \rightarrow Cu(CH_3COO)_2 + H_2O \quad (2)$$

$$Cu_2O + 4CH_3COOH \rightarrow 2Cu(CH_3COO)_2 + H_2O + H_2 \quad (3)$$

Nanocopper foams were first characterized five days after dealloying of the copper silicide by XPS analysis, to check for the presence of native oxides. A Thermo Scientific Thermo K-alpha XPS tool having a base pressure of $< 3 \times 10^{-9}$ Torr and fitted with a monochromatic Al Kα (1486.6 eV) X-ray source with a hemispherical analyzer was used in this study. Bulk Cu samples were characterized along with, serving as reference to validate the method. XPS analysis detected Cu, O, C and trace Si in the survey spectra, while typical native oxide signature can be identified from the strong satellites (shake-up peaks) characteristic of CuO [66] from the Cu 2p scan spectra in both as-dealloyed foam and bulk Cu samples. The Cu 2p peak positions represent the binding energy required for an electron in the 2p shell of copper to be ejected as a photoelectron. Both samples were then immersed in glacial acetic acid (>99.85% Sigma Aldrich) without any further dilutions, at room temperature, for two minutes. Post-acid-exposed surfaces were then dried with a N_2 gas gun. Acetic

acid has low surface tension (27.8 dyn/cm), allowing easy removal from the surface. After acetic acid treatment, the pure copper Cu 2p peaks, Cu $2p_{3/2}$ (932.6 eV) and Cu $2p_{1/2}$ (952.4 eV), dominated the spectra for both bulk and nanocopper foams as can be seen from Fig. 3(a)-(b).

Carbon contamination is generally unavoidable when dealing with samples in ambient air conditions. For oxidized samples, the C 1s peak generally has two components: the adventitious carbon peak, as well as the carboxylate peak. On comparing the C 1s peak, it was observed that the carboxylate peak disappears on treatment with acetic acid, thus agreeing with observations from reported studies on copper oxide reduction [65]. We note that in a previous study of similarly synthesized NP copper high-resolution TEM failed to detect presence of oxide in the examined samples [67]. An apparent contradiction of TEM analysis and the XPS data presented here merits a further examination. Regardless of the origin of oxides detected by XPS, a simple method for oxide removal by acetic acid treatment has thus been demonstrated here. Acetic acid treatment had no discernible effect on the foam nanostructure, and resulted in no contamination from residual acid on account of its low surface tension.

C. DSC Characterization

Thermal coarsening studies conducted on nanogold foams revealed that the nano-sized ligaments tended to thicken upon thermal annealing at temperatures much lower than the melting point of Au. This suggests the possibility of a low-temperature solid-state growth mechanism that brings about coarsening of the foams rather than conventional melting to liquid phase. To understand the endo- and exothermic behavior of nanocopper foams, a DSC study was carried out on an as-dealloyed sample on Si substrate in a standard alumina pan using a Thermal Analysis – SDT Q600 DSC instrument. The sample mass was 8.59 milligrams. The heating rate for the experiment was set at 20K/min. The DSC was conducted under constant N_2 flow. Fig. 4 shows the DSC result for a nanocopper foam.

Typically, an endothermic peak is seen for first order melting phenomena, and this peak corresponds to the melting point of the nanoscale sample. However, in the present case, an exothermal peak is visible at 183ºC. The heat released (stored energy) during the exothermal reaction can be calculated as 12.24 J/gm matching closely to that reported for nanoporous gold of 11 J/gm [68]. The presence of this exothermal peak at such low temperature of 0.2 T/T_m indicates that there may be a solid-state strain-release occurring in the nanocopper foam that could be attributed to coarsening of the ligaments. The high surface-to-volume ratio in such foams may have triggered a recovery-like process or recrystallization that initiated coarsening of the foam.

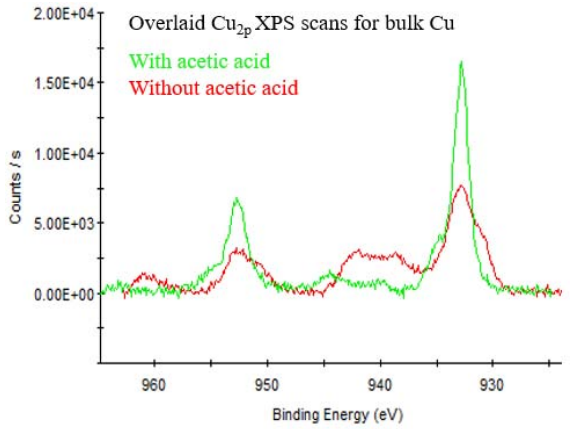

(a)

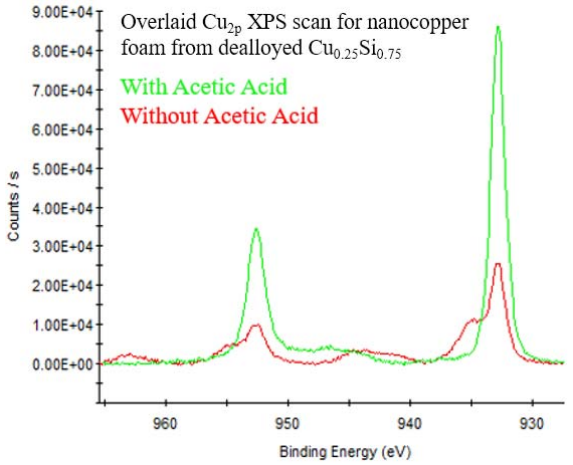

(b)

Figure 3. Overlaid Cu_{2p} XPS scan of (a) bulk Cu, and (b) dealloyed nanocopper foams; as-fabricated and after acetic acid treatment.

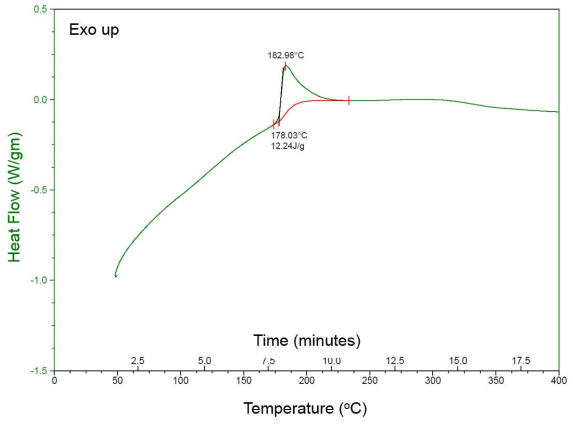

Figure 4. Differential scanning calorimetry plot of as-dealloyed nanocopper foam on Si substrate

Further investigation is required to fully understand the nature of recrystallization and hence, explain the coarsening mechanisms in nanocopper foams. A preliminary sintering study was finally carried out to corroborate the results from this DSC experiment.

III. Sintering of Nanocopper Foams

Sintering studies were conducted by subjecting as synthesized nanocopper foam samples to thermal treatment at 150°C and 300°C, respectively, for 180-900sec. A rapid thermal annealing furnace (SSI – RTP) was used for better temperature control with a ramp rate of 30°C/sec. The atmosphere within the chamber was controlled to 5 SLM of N_2 gas flow to ensure minimal presence of air in the chamber, and thus limit potential oxidation of the foams during thermal annealing. Fig. 5 shows FE – SEM images of the thermally treated nanocopper foams. The average ligament size for foams that were heat-treated at 150°C for 180sec is about 46nm measured over 25 measurements, with an overall foam thickness averaging 1.55µm. The ligament dimensions are similar to room-temperature measurements on the nanocopper foams to within 2%, while the cross-sectional morphology of the aged foams, shown in Fig. 5(c)-(d), closely matches that of as-dealloyed samples from Fig. 5(a)-(b), shown for comparison.

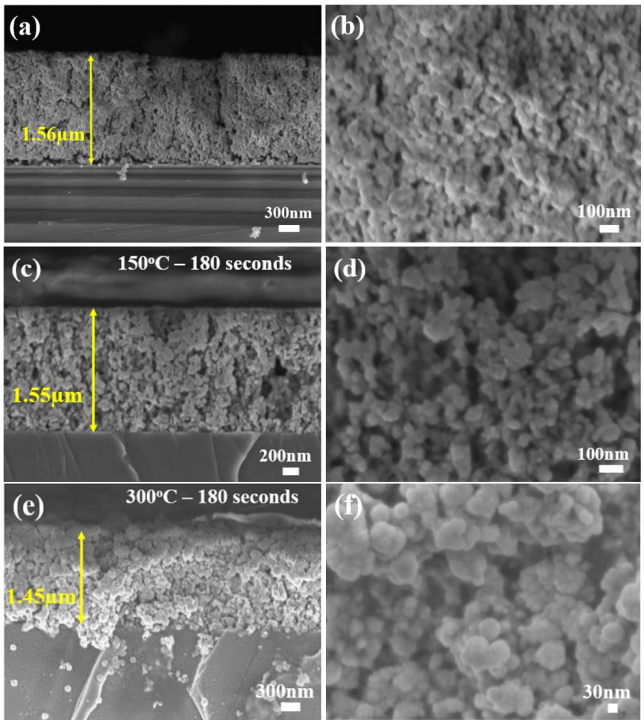

Figure 5. Cross-sectional FE-SEM micrographs of thermally treated nanocopper foam layers in the following conditions: (a) as-dealloyed, (b) as-dealloyed magnified view, (c) 150°C – 180sec, (d) 150°C – 180sec magnified view, (e) 300°C – 180sec, (f) 300°C – 180sec magnified view.

This suggests that little to no coarsening occurred in the foams at 150°C. However, upon heat treatment at 300°C for 180sec, the average NP Cu thickness decreased to 1.45µm while the average ligament size increased to 60nm. It can be seen from Fig. 5(e)-(f) that the ligaments are beginning to fuse with each other, thus isolating the pores, and the morphology is moving towards a densified structure.

Maintaining a 300°C temperature, the foams were then further heat treated for a longer duration of 900sec, to observe the effect of time on the coarsening behavior. Fig. 6(a) shows large scale fusion with an evolution in necking of the ligaments, giving rise to thickened nodes and an overall shrinkage of the nanocopper foam to 1.37µm thickness. The average ligament size also increased to 65nm with intermittent continuous Cu phases across the height of the foam. The nanocopper foam appears to be partially densified from the plan-view images in Fig. 6(b) as compared to plan-view of the as-dealloyed foam from Fig. 2(d).

From these initial experiments, it can be concluded that the studied nanocopper foams did not undergo significant coarsening at 150°C, with slight shrinkage and morphological changes as compared to the as-dealloyed samples. However, upon heat treatment at 300°C, more substantial coarsening of nanocopper ligaments was observed along with further shrinkage. This correlates well with the data from the DSC characterization and suggests it may be due to a recrystallization-based solid-state reaction that occurs at around 180°C. This reaction activates surface diffusion of copper along the ligaments and initiates the coarsening mechanism. While this empirical study correlates well with thermal coarsening of nanoporous gold suggesting the formation of a disconnected closed-pore structure with coarsening and densification occurring beyond 200°C [69], a more detailed analysis of coarsening and densification kinetics is required to fully understand the behavior of nanocopper foams, towards their use as interconnection materials.

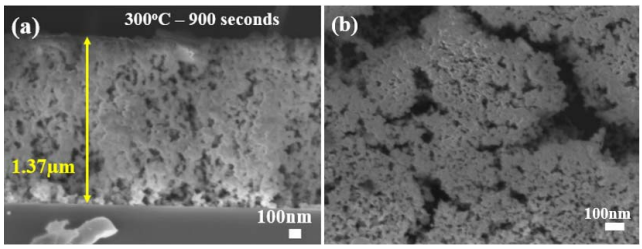

Figure 6. FE-SEM micrographs of nanocopper foam layer thermally treated at 300°C – 900sec: (a) 90° tilt view, (b) Plan-view

IV. Summary and Conclusions

This paper presents the first demonstration of an all-Cu interconnection technology based on sintering of nanocopper foams. Nanocopper foam properties are strongly dependent on the initial alloy composition, fabrication conditions and

morphology, thus allowing design flexibility in tuning the physical properties towards a wide range of applications. Nanocopper foams with ligament size of 45nm were fabricated by dealloying amorphous $Cu_{0.25}Si_{0.75}$ in hydrofluoric acid. The as-dealloyed foam had an open-cell structure consisting of a 3D bi-continuous network of interconnected ligaments. A preliminary oxidation study was conducted with XPS characterization, indicating the presence of native oxides that were effectively removed by acetic acid treatment. DSC characterization of these foams revealed the presence of a solid-state recrystallization reaction between 178 – 210°C, suggesting initiation of coarsening and growth from these temperatures. Isothermal heating of oxide-free nanocopper foams at 150°C and 300°C agreed well with the DSC results, with no substantial coarsening occurring at 150°C. In contrast, at 300°C there was substantial densification. These results suggest the possible presence of a temperature-based activation barrier towards surface diffusion in nano-Cu ligaments that lead to thermal coarsening and densification in the final stages.

Consequently, nanocopper foams constitute a promising low-cost interconnection material for direct Cu-Cu bonding at temperatures below 250°C, with improved manufacturability and tolerance to non-coplanarities. Further investigation is merited on different fabrication routes and their subsequent effect on the physical properties of the synthetized foams, as well a fundamental understanding of oxidation and sintering kinetics. This research will provide guidelines for material design with foams customized to the target application, be it consumer, high-performance or automotive. Nanocopper foam-based interconnections have therefore the potential to become a disruptive technology that changes the interconnection landscape in the years to come.

ACKNOWLEDGMENTS

This study was supported by the Interconnections and Assembly (I&A) industry program at Georgia Tech PRC. The authors are grateful to the industry sponsors and mentors for their funding and technical guidance. Cu-Si alloy deposition was performed at the Center for Integrated Nanotechnologies, an Office of Science User Facility operated for the U.S. Department of Energy (DOE) Office of Science by Los Alamos National Laboratory (Contract DE-AC52-06NA25396).

REFERENCES

[1] P. Totta, "History of Flip Chip and Area Array Technology," in *Area Array Interconnection Handbook*, K. Puttlitz and P. Totta, Eds., ed: Springer US, 2001, pp. 1-35.

[2] K. Suganuma, S.-J. Kim, and K.-S. Kim, "High-temperature lead-free solders: Properties and possibilities," *JOM,* vol. 61, pp. 64-71, 2009.

[3] Z. X. Zhu, C. C. Li, L. L. Liao, C. K. Liu, and C. R. Kao, "Au–Sn bonding material for the assembly of power integrated circuit module," *Journal of Alloys and Compounds,* vol. 671, pp. 340-345, 6/25/ 2016.

[4] H. A. Mustain, W. D. Brown, and S. S. Ang, "Transient Liquid Phase Die Attach for High-Temperature Silicon Carbide Power Devices," *Components and Packaging Technologies, IEEE Transactions on,* vol. 33, pp. 563-570, 2010.

[5] S. Fu, Y. Mei, G.-Q. Lu, X. Li, G. Chen, and X. Chen, "Pressureless sintering of nanosilver paste at low temperature to join large area (⩾ 100 mm2) power chips for electronic packaging," *Materials Letters,* vol. 128, pp. 42-45, 8/1/ 2014.

[6] T. Wang, X. Chen, G.-Q. Lu, and G.-Y. Lei, "Low-Temperature Sintering with Nano-Silver Paste in Die-Attached Interconnection," *Journal of Electronic Materials,* vol. 36, pp. 1333-1340, 2007/10/01 2007.

[7] N. Heuck, K. Guth, M. Thoben, A. Mueller, N. Oeschler, L.Boewer*, et al.*, "Aging of new Interconnect-Technologies of Power-Modules during Power-Cycling," in *Integrated Power Systems (CIPS), 2014 8th International Conference on*, 2014, pp. 1-6.

[8] K. Guth, N. Oeschler, L. Boewer, R. Speckels, G. Strotmann, N. Heuck*, et al.*, "New assembly and interconnect technologies for power modules," in *Integrated Power Electronics Systems (CIPS), 2012 7th International Conference on*, 2012, pp. 1-5.

[9] K. Guth, "New assembly and interconnects beyond sintering methods PCIM 2010," *Nuremberg, Germany*.

[10] Go, x, C. bl, and J. Faltenbacher, "Low temperature sinter technology die attachment for power electronic applications," in *Integrated Power Electronics Systems (CIPS), 2010 6th International Conference on*, 2010, pp. 1-5.

[11] Y. Hino, N. Yokomura, and H. Tatsumi, "Packaging Technologies for High-Temperature Power Semiconductor Modules."

[12] R. Agarwal, W. Zhang, P. Limaye, R. Labie, B. Dimcic, A. Phommahaxay*, et al.*, "Cu/Sn microbumps interconnect for 3D TSV chip stacking," in *Electronic Components and Technology Conference (ECTC), 2010 Proceedings 60th*, 2010, pp. 858-863.

[13] K. Zeng, R. Stierman, T.-C. Chiu, D. Edwards, K. Ano, and K. N. Tu, "Kirkendall void formation in eutectic SnPb solder joints on bare Cu and its effect on joint reliability," *Journal of Applied Physics,* vol. 97, p. 024508, 2005.

[14] C. F. Luk, Y. C. Chan, and K. C. Hung, "Development of gold to gold interconnection flip chip bonding for chip on suspension assemblies," *Microelectronics Reliability,* vol. 42, pp. 381-389, 3// 2002.

[15] G. G. Zhang, X. F. Ang, Z. Chen, C. C. Wong, and J. Wei, "Critical temperatures in thermocompression gold stud bonding," *Journal of Applied Physics,* vol. 102, p. 063519, 2007.

[16] Y. H. Hu, C. S. Liu, M. J. Lii, K. J. Rebibis, A. Jourdain, A. L. Manna*, et al.*, "3D stacking using Cu-Cu direct bonding," in *3D Systems Integration Conference (3DIC), 2011 IEEE International*, 2012, pp. 1-4.

[17] Y.-S. Tang, Y.-J. Chang, and K.-N. Chen, "Wafer-level Cu–Cu bonding technology," *Microelectronics Reliability,* vol. 52, pp. 312-320, 2// 2012.

[18] N. Shahane, S. McCann, G. Ramos, A. Killian, R. Taylor, V. Sundaram*, et al.*, "Modeling, design and demonstration of low-temperature, low-pressure and high-throughput thermocompression bonding of copper interconnections without solders," in *Electronic Components and Technology Conference (ECTC) , 2015 IEEE 65th*, 2015, pp. 1859-1865.

[19] J. Zurcher, K. Yu, G. Schlottig, M. Baum, M. M. Visser Taklo, B. Wunderle*, et al.*, "Nanoparticle assembly and sintering towards all-copper flip chip interconnects," in *Electronic Components and Technology Conference (ECTC) , 2015 IEEE 65th*, 2015, pp. 1115-1121.

[20] K. S. Siow, "Are Sintered Silver Joints Ready for Use as Interconnect Material in Microelectronic Packaging?," *Journal of Electronic Materials,* vol. 43, pp. 947-961, 2014.

[21] K. Schnabl, L. Wentlent, K. Mootoo, S. Khasawneh, A. A. Zinn, J. Beddow*, et al.*, "Nanocopper Based Solder-Free Electronic Assembly," *Journal of Electronic Materials,* vol. 43, pp. 4515-4521, 2014/12/01 2014.

[22] N. Mizumura and K. Sasaki, "Development of low-temperature sintered nano-silver pastes using MO technology and resin reinforcing technology," in *Electronics Packaging (ICEP), 2014 International Conference on*, 2014, pp. 526-531.

[23] J. R. Calvert DC, "XLI.—Action of acids upon metals and alloys," *Journal of the Chemical Society,* vol. 19, pp. 434 - 454, 1866.

[24] A. J. Forty, "Corrosion micro-morphology of noble-metal alloys and depletion gilding " *Nature,* vol. 282, pp. 597-598, 1979.

[25] R. Li and K. Sieradzki, "Ductile-brittle transition in random porous Au," *Physical Review Letters,* vol. 68, pp. 1168-71, 1992.

[26] S. G. Corcoran, D. Wiesler, J. Barker, and K. Sierradzki, "In situ small angle neutron scattering investigation of $Ag_{0.7}Au_{0.3}$ dealloying," *Materials Research Society Symposium Proceedings,* vol. 376, pp. 377-382, November 28 - December 1, 1994 1995.

[27] K. Wagner, S. R. Brankovic, N. Dimitrov, and K. Sieradzki, "Dealloying below the critical potential," *Journal of the Electrochemical Society,* vol. 144, pp. 3545-55, 1997.

[28] J. Erlebacher and K. Sieradzki, "Pattern formation during dealloying," *Scripta Materialia,* vol. 49, pp. 991-6, 2003.

[29] D. Yi, K. Young-Ju, and E. Jonah, "Nanoporous gold leaf: "Ancient technology"/advanced material," *Advanced Materials,* vol. 16, p. 4, November 4 2004.

[30] S. Parida, D. Kramer, C. A. Volkert, H. Rosner, J. Erlebacher, and J. Weissmuller, "Volume change during the formation of nanoporous gold by dealloying," *Physical Review Letters,* vol. 97, pp. 035504-4, 2006.

[31] Z. Qi, C. Zhao, X. Wang, J. Lin, W. Shao, Z. Zhang*, et al.*, "Formation and Characterization of Monolithic Nanoporous Copper by Chemical Dealloying of Alâ`Cu Alloys," *The Journal of Physical Chemistry C,* vol. 113, pp. 6694-6698, 2009.

[32] A. J. Forty and P. Durkin, "A micromorphological study of the dissolution of silver-gold alloys in nitric acid," *Philosophical Magazine A (Physics of Condensed Matter, Defects and Mechanical Properties),* vol. 42, pp. 295-318, 1980.

[33] J. Biener, A. M. Hodge, J. R. Hayes, C. A. Volkert, L. A. Zepeda-Ruiz, A. V. Hamza*, et al.*, "Size effects on the mechanical behavior of nanoporous Au," *Nano Letters,* vol. 6, pp. 2379-2382, 2006.

[34] C. A. Volkert, E. T. Lilleodden, D. Kramer, and J. Weissmuller, "Approaching the theoretical strength in nanoporous Au," *Applied Physics Letters,* vol. 89, pp. 61920-1, 2006.

[35] D. Lee, X. D. Wei, M. H. Zhao, X. Chen, S. C. Jun, J. Hone*, et al.*, "Plastic deformation in nanoscale gold single crystals and open-celled nanoporous gold," *Modelling and Simulation in Materials Science and Engineering,* vol. 15, pp. S181-S192, May 21-25, 2006 2007.

[36] X. Lu, T. J. Balk, R. Spolenak, and E. Arzt, "Dealloying of Au-Ag thin films with a composition gradient: Influence on morphology of nanoporous Au," *Thin Solid Films,* vol. 515, pp. 7122-7126, 2007.

[37] J. T. Zhang, P. P. Liu, H. Y. Ma, and Y. Ding, "Nanostructured porous gold for methanol electro-oxidation," *Journal of Physical Chemistry C,* vol. 111, pp. 10382-10388, 2007.

[38] D. V. Pugh, A. Dursun, and S. G. Corcoran, "Formation of nanoporous platinum by selective dissolution of Cu from Cu{sub 0.75}Pt{sub 0.25}," *Journal of Materials Research,* vol. 18, pp. 216-21, 2003.

[39] J. C. Thorp, K. Sieradzki, L. Tang, P. A. Crozier, A. Misra, M. Nastasi*, et al.*, "Formation of nanoporous noble metal thin films by electrochemical dealloying of Pt{sub x}Si{sub 1-x}," *Applied Physics Letters,* vol. 88, pp. 1-3, 2006.

[40] L. Y. a. A. Antonia, "Synthesis of transversely isotropic nanoporous platinum," *Scripta Materialia,* vol. in press, 2011.

[41] A. Antoniou, D. Bhattacharrya, J. K. Baldwin, P. Goodwin, M. Nastasi, S. T. Picraux*, et al.*, "Controlled nanoporous Pt morphologies by varying deposition parameters," *Applied Physics Letters,* vol. 95, 2009.

[42] J. R. Hayes, A. M. Hodge, J. Biener, A. V. Hamza, and K. Sieradzki, "Monolithic nanoporous copper by dealloying Mn-Cu," *Journal of Materials Research,* vol. 21, pp. 2611-16, 2006.

[43] Z. Qi, C. Zhao, X. Wang, J. Lin, W. Shao, Z. Zhang*, et al.*, "Formation and Characterization of Monolithic Nanoporous Copper by Chemical Dealloying of Al−Cu Alloys," *The Journal of Physical Chemistry C,* vol. 113, pp. 6694-6698, 2009/04/23 2009.

[44] I. C. Cheng and A. M. Hodge, "Morphology, Oxidation, and Mechanical Behavior of Nanoporous Cu Foams," *Advanced Engineering Materials,* pp. n/a-n/a, 2011.

[45] H. Liu, P. He, Z. Li, and J. Li, "High surface area nanoporous platinum: facile fabrication and electrocatalytic activity," *Nanotechnology,* vol. 17, p. 2167, 2006.

[46] R. Wang, C. Wang, W. B. Cai, and Y. Ding, "Ultralow‐Platinum‐Loading High‐Performance Nanoporous Electrocatalysts with Nanoengineered Surface Structures," *Advanced Materials,* vol. 22, pp. 1845-1848, 2010.

[47] X. Peng, K. Koczkur, S. Nigro, and A. Chen, "Fabrication and electrochemical properties of novel nanoporous platinum network electrodes," *Chem. Commun.,* pp. 2872-2873, 2004.

[48] V. Zielasek, B. Jürgens, C. Schulz, J. Biener, M. M. Biener, A. V. Hamza*, et al.*, "Gold catalysts: nanoporous gold foams," *Angewandte Chemie International Edition,* vol. 45, pp. 8241-8244, 2006.

[49] A. Wittstock, V. Zielasek, J. Biener, C. Friend, and M. Bäumer, "Nanoporous gold catalysts for selective gas-phase oxidative coupling of methanol at low temperature," *Science,* vol. 327, pp. 319-322, 2010.

[50] R. Zeis, T. Lei, K. Sieradzki, J. Snyder, and J. Erlebacher, "Catalytic reduction of oxygen and hydrogen peroxide by nanoporous gold," *Journal of Catalysis,* vol. 253, pp. 132-138, 2008.

[51] T. Fujita, P. Guan, K. McKenna, X. Lang, A. Hirata, L. Zhang*, et al.*, "Atomic origins of the high catalytic activity of nanoporous gold," *Nature materials,* vol. 11, pp. 775-780, 2012.

[52] N. Asao, Y. Ishikawa, N. Hatakeyama, Y. Yamamoto, M. Chen, W. Zhang*, et al.*, "Nanostructured Materials as Catalysts: Nanoporous‐Gold‐Catalyzed Oxidation of Organosilanes with Water," *Angewandte Chemie International Edition,* vol. 49, pp. 10093-10095, 2010.

[53] N. Kranzlin and M. Niederberger, "Controlled fabrication of porous metals from the nanometer to the macroscopic scale," *Materials Horizons,* vol. 2, pp. 359-377, 2015.

[54] J. R. Hayes, A. M. Hodge, J. Biener, A. V. Hamza, and K. Sieradzki, "Monolithic nanoporous copper by dealloying Mn–Cu," *Journal of Materials Research,* vol. 21, pp. 2611-2616, 2006.

[55] R. Liu, S. Zheng, J. Kevin Baldwin, M. Kuthuru, N. Mara, and A. Antoniou, "Synthesis and mechanical behavior of nanoporous nanotwinned copper," *Applied Physics Letters,* vol. 103, p. 241907, 2013.

[56] Q. Yang, S. Liang, B. Han, J. Wang, and R. Mao, "Preparation and properties of enhanced bulk nanoporous coppers," *Materials Letters,* vol. 73, pp. 136-138, 4/15/ 2012.

[57] J. Li, H. Jiang, N. Yu, C. Xu, and H. Geng, "Fabrication and characterization of bulk nanoporous copper by dealloying Al–Cu alloy slices," *Corrosion Science,* vol. 90, pp. 216-222, 1// 2015.

[58] X. Luo, R. Li, L. Huang, and T. Zhang, "Nucleation and growth of nanoporous copper ligaments during electrochemical dealloying of Mg-based metallic glasses," *Corrosion Science,* vol. 67, pp. 100-108, 2// 2013.

[59] H.-B. Lu, Y. Li, and F.-H. Wang, "Synthesis of porous copper from nanocrystalline two-phase Cu–Zr film by dealloying," *Scripta Materialia,* vol. 56, pp. 165-168, 1// 2007.

[60] R. Liu and A. Antoniou, "A relation between relative density, alloy composition and sample shrinkage for nanoporous metal foams," *Scripta Materialia,* vol. 67, pp. 923-926, 12// 2012.

[61] L. Kecheng, L. Xiaogang, C. Mingxiang, and L. Sheng, "Research on nano-thermocompression bonding process using nanoporous copper as bonding layer," in *Electronic Packaging Technology (ICEPT), 2014 15th International Conference on*, 2014, pp. 19-23.

[62] R. Liu and A. Antoniou, "Influence of dealloying parameters on the elastic response of nanoporous copper," *in preparation*.

[63] I. McCue, E. Benn, B. Gaskey, and J. Erlebacher, "Dealloying and Dealloyed Materials," *Annual Review of Materials Research,* vol. 46, p. null, 2016.

[64] W. Liu, L. Chen, J. Yan, N. Li, S. Shi, and S. Zhang, "Dealloying solution dependence of fabrication, microstructure and porosity of hierarchical structured nanoporous copper ribbons," *Corrosion Science,* vol. 94, pp. 114-121, 5// 2015.

[65] H. G. Tompkins and D. L. Allara, "The study of the gas—solid interaction of acetic acid with a cuprous oxide surface using

reflection—absorption spectroscopy," *Journal of Colloid and Interface Science,* vol. 49, pp. 410-421, 12// 1974.
[66] J. F. Moulder, J. Chastain, and R. C. King, *Handbook of X-ray photoelectron spectroscopy: a reference book of standard spectra for identification and interpretation of XPS data*: Physical Electronics Eden Prairie, MN, 1995.
[67] R. Liu, S. Zheng, J. K. Baldwin, M. Kuthuru, N. Mara, and A. Antoniou, "Synthesis and mechanical behavior of nanoporous nanotwinned copper," *Applied Physics Letters,* vol. 103, p. 241907, 2013.
[68] M. Hakamada and M. Mabuchi, "Thermal coarsening of nanoporous gold: Melting or recrystallization," *Journal of Materials Research,* vol. 24, pp. 301-304, 2009.
[69] R. N. Viswanath, V. A. Chirayath, R. Rajaraman, G. Amarendra, and C. S. Sundar, "Ligament coarsening in nanoporous gold: Insights from positron annihilation study," *Applied Physics Letters,* vol. 102, p. 253101, 2013.